Article

Shear Stud Bonds in a Contact Joint of Steel-Concrete Beams

Farit Zamaliev * and Ashot Tamrazyan *

Posted Date: 27 December 2023

doi: 10.20944/preprints202312.2029.v1

Keywords: steel-reinforced concrete structures; anchor connections; anchor strength; analytical dependencies; shear studs bond

Article

Shear Stud Bonds in a Contact Joint of Steel-Concrete Beams

Farit Zamaliev [1,*] and Ashot Tamrazyan [2,*]

[1] Kazan State University of Architecture and Engineering, Kazan, Russian Federation; zamaliev49@mail.ru
[2] Moscow State University of Civil Engineering, Moscow, Russian Federation; tamrazian@mail.ru
* Correspondence: zamaliev49@mail.ru; Tel.: +79872960949

Abstract: The research object was the stress-strain state of shear stud bonds in the contact joint of steel-concrete beams. The work diagrams for three types of anchors are given. Based on the analysis of numerical and full-scale experiments, analytical dependencies are proposed that reflect the actual operation of anchor ties. Comparisons of the calculation results by analytical formulas and comparisons with numerical and full-scale experiment data are given. Numerical studies have revealed the pattern of the stress-strain state of the contact joint, the stages of development of cracks in the concrete flange, and the sequence of development of deformations in anchor ties. It was revealed that vertical shear studs bonds have an increased bearing capacity, although displacements are 1.5-2 times greater than those of loop-shaped anchor ties.

Keywords: steel-reinforced concrete structures; anchor connections; anchor strength; analytical dependencies; shear studs bond

1. Introduction

In steel-concrete beams and slabs, which are structures of a composite section, one of the main issues is ensuring reliable joint operation of the layers provided by anchor ties [1]. A correct assessment of the bearing capacity of anchor ties makes it possible to design reliable and economical steel-reinforced concrete structures of a composite section consisting of two or more layers [2].

The steel-concrete composite beam with non-welded horizontal shear connectors subjected to static bending has been studied [3]. The test outcomes demonstrate a behavior akin to steel-concrete composite beams with conventional connectors. In this context, a flexural failure manifested itself, forming a plastic hinge within the mid-span cross-section. This phenomenon was concomitant with the yielding of the steel girder and the concrete's compression. Consequently, it is worth noting that the connection under examination exhibited remarkable resilience, as it effectively facilitated the transmission of shear forces from the slab to the girder throughout the duration of the test.

A steel-concrete composite beam with shear studs was loaded under a monotonic bending moment until failure [4]. Prior to the commencement of the test, the concrete segment of the beam displayed transverse cracking, primarily attributable to constrained shrinkage strains. The behavior of the beam can be categorized into two distinct domains: an elastic phase and a plastic phase, characterized by substantial ductility. The central region experienced failure due to high compressive strains within the concrete component, eventually leading to its crushing. Notably, the initial transverse cracks introduced significant discontinuities in the longitudinal slip distribution, particularly within the elastic phase, and also brought about a noticeable transformation in the deflection pattern of the shear studs within the concrete slab. Numerical simulations conducted within the elastic domain, accounting for slip or its absence, closely aligned with experimental measurements in terms of deflection and longitudinal strains.

Numerical studies and comparisons with the results of experimental studies of steel-reinforced concrete beams with studs at the junction of layers are given in the source [5]. A steel-concrete beam was tested under cyclic loading and showed no fatigue damage after over 2 million cycles. The beam

 doi:10.20944/preprints202312.2029.v1

was then statically loaded up to failure. Its behavior within the elastic and plastic domain was very similar to that of the same beam previously subjected to static loading only. However, analytical expressions for estimating the strength of studs were not presented.

The outcomes of numerous experiments involving composite beams containing trapezoidal steel decking are showcased and complemented by the results of corresponding pushout tests [6]. A comprehensive examination of the shear connection's performance is undertaken, considering both meticulously executed pushout tests without applying supplementary lateral restraints and beam tests. This scrutiny revealed that the failure modes observed in both types of tests were congruent, the load-slip characteristics exhibited remarkable similarity, and the strengths of the connectors were comparable.

The articles [7] and [8] studied the dynamic behavior of steel-concrete composite beams with differing shear connection systems. Two distinct blind bolt connectors were employed as shear connection systems within steel-concrete composite beams. A comprehensive Timoshenko beam model designed for steel-concrete composite beams was established and subsequently juxtaposed with the outcomes of practical experiments. Furthermore, an exploration was conducted using the Timoshenko beam model to scrutinize an uncertain boundary condition. As a result of this investigation, an empirical correlation was formulated, establishing a connection between the displacements observed at the beam supports and the rotation of the cross-sectional face. A finite element model was then developed. The nature of changes in dynamic behavior due to damage was investigated using the finite element model. It was found that at increased loading, the behavior of the cast-in and retrofitted connectors was fundamentally different due to the retrofitting procedure.

An in-depth exploration was conducted into the dynamic characteristics of steel-concrete composite beams that had undergone retrofitting with various bolted shear connectors [9]. An experimental investigation focused on cast-in versus retrofitted shear connectors to unveil the distinctions in their dynamic performance. This study involved identical steel-concrete composite beams equipped with diverse shear connection systems. The research encompassed using two types of blind bolt connectors as shear connection systems within the steel-concrete composite beams. Additionally, a welded shear stud specimen was examined in cast-in and retrofitted configurations for comprehensive analysis. Subsequently, a finite element model was meticulously crafted to facilitate a deeper understanding of the alterations in dynamic behavior associated with damage.

In 2018, the research of steel-concrete trussed beams with a steel joist with inclined rebars, which are welded to a smooth steel plate and then embedded within the concrete cast in situ, was reviewed [10]. The most relevant scientific contributions published up to 2018 regarding the experimental investigation of shear behavior were summarized and discussed. The codes and analytical models are reviewed.

The steel-concrete composite beams with the perfobond shear connectors (PSCs) were studied [11]. Ten one-sided pull-out tests have been conducted to investigate the PSC's behavior and shear resistance. The results were compared against pull-out test results from other researchers and the predictions offered by several shear resistance equations. It has been found that the one-sided pull-out test results are consistent with the analytical predictions offered by these expressions compared to the previous research using pull-out tests.

The article [12] studies a composite steel-concrete bridge floor featuring headed shear studs affixed to a flat steel plate. It is expected to combine thick steel plates with a relatively moderate layer of concrete in bridge construction. In some instances, particularly in wide slab applications, the optimal arrangement for the placement of shear studs may necessitate their welding on top of an existing butt weld between steel plates. An intriguing aspect of this scenario is our limited knowledge regarding the shear resistance at the weld-to-weld interface and its potential adverse effects on the overall system's resistance. Additionally, the ultimate behavior of this system involves a combination of factors. It initially hinges on the flexural resistance of a composite cross-section. However, when the concrete experiences cracking, it transitions into developing a compressed arch anchored in the headed shear studs. This transition highlights the critical importance of these connections. The research paper delves into these critical inquiries and offers an exhaustive analysis of the system's

 doi:10.20944/preprints202312.2029.v1

behavior when it reaches its ultimate limit state. The investigation includes two types of tests. The first category comprises pure shear tests that align with pushout tests, while the second category involves beam tests subject to four-point loading, where the shear spans bear longitudinal shear loads. In each pair of tests, a reference specimen is prepared. These specimens either lack a butt weld or include a butt weld directly beneath the line of shear studs. Notably, the study focuses on typical floor dimensions relevant to bridge applications.

The lockbolt demountable shear connector (LB-DSC) has been introduced [13]. The described connector presents a design in which a steel tube filled with grout is securely integrated into a concrete slab and is fastened to a partial-thread bolt with precise geometric compatibility. This bolt is anchored to the upper flange of a steel section in a composite beam. A distinctive feature of this design is the incorporation of a conical seat lug that firmly engages with a predrilled, counter-sunk hole in the flange of the steel section, ensuring a slip-free connection between the bolt and the flange. The deconstruction process of the lockbolt demountable shear connector is straightforward, involving the use of a specially modified wrench to disengage the tube from the top of the slab. Pushout tests have demonstrated exceptional shear resistance and stiffness compared to alternative demountable shear connectors. The results pertaining to slip capacity further classify the lockbolt demountable shear connector as a ductile shear connector, significantly enhancing its desirability for use in structural applications. A design equation has been developed based on an extensive analysis involving numerical simulations and experimental findings. This equation enables the prediction of shear resistance for the lockbolt demountable shear connector, offering a valuable tool for engineers and designers in the field.

The research [14] examined the load-bearing capacity of shear stud connectors. It entailed applying finite element analysis through ABAQUS software to replicate the force-deformation behavior of these shear studs. Pushout tests were conducted to validate the accuracy of the finite element model. The investigation was then extended through comprehensive parametric numerical studies, which aimed to scrutinize the force-deformation attributes of diverse shear stud configurations. As a result of these endeavors, a design equation was formulated employing linear regression techniques, using the insights gleaned from the parametric studies. Notably, this derived equation exhibited a commendable degree of conformity with the empirical data obtained from the experimental assessments.

In the context of research [15], a novel and cutting-edge shear connector involving bolts for steel-concrete composite structures was introduced. A series of static push-off tests were conducted to evaluate its performance, considering various bolt dimensions, the constrained condition of reserved holes, and the dimensions of the slab holes. Subsequently, a finite element model was validated using the experimental data. This model was further employed to explore the impact of concrete strength, bolt dimensions, yield strength, bolt pretension, and the length-to-diameter ratio of high-strength bolts on the shear connector's performance. Based on the insights from finite element simulations and test results, approximation formulas for assessing the shear resistance behavior were proposed.

Compared to conventional concrete, the coconut shell concrete in steel-concrete-steel sandwich beams under flexure was studied [16]. Two cases without and with shear studs were considered to interconnect the bottom tension and top compression plates. The effect of river sand replaced with quarry dust was also considered. Therefore, four mixes of conventional concrete, conventional concrete produced using quarry dust, coconut shell concrete, and coconut shell concrete produced using quarry dust were used. Three different steel plate thicknesses were considered (4 mm, 6 mm, and 8 mm). Twelve steel-concrete-steel specimens were tested to evaluate the flexural performance under two-point static loads. It was found that the moment carrying capacity of the steel-concrete-steel sandwich beams increased when the thickness of the steel plate increased. Using quarry dust to replace river sand augmented the strength of beams.

In [17], a comprehensive investigation was conducted using a three-dimensional finite element model to assess the performance of high-strength bolted shear connectors under inverse push-off loading conditions. The finite element model was thoughtfully constructed to incorporate material nonlinearities and interactions among all constituent elements. Initial validation was performed

 doi:10.20944/preprints202312.2029.v1

against available push-off test results to establish the credibility and precision of the proposed finite element model. Subsequently, a parametric study was undertaken to delineate the influence of various factors, including concrete strength, bolt diameter, bolt tensile strength, clearance between the concrete slab and the bolt, and bolt pretension, on the shear performance of high-strength bolted shear connectors. As a result of this study, design recommendations were formulated to facilitate the estimation of the shear load at the point of first slip and the load-bearing capacity of high-strength bolted shear connectors.

In addition to the aforementioned investigation, steel-concrete-steel sandwich panels were scrutinized. These panels featured two thin high-strength steel plates enveloping a moderately low-density and low-strength thick concrete core [18]. A stud-bolt connector was used to regulate its shear behavior in sandwich panels. The parameters under analysis were the bolts' diameter, the concrete core's thickness, and the bolts' spacing. Furthermore, the concrete core was manufactured with normal-strength concrete and steel fibers concrete. An approximation formula was proposed to determine the shear strength.

A multi-cavity steel-concrete composite beam was proposed [19]. This beam used an internal perforated steel plate to connect the concrete with the steel structure instead of shear connectors. Two beams with the angle of inner porous steel plate as 60° and 75° were tested. The finite element modeling was used to analyze the influence of concrete strength, steel strength, porosity, and the angle of internal porous steel plate on the mechanical properties of composite beams. The bearing capacity of the composite beam is positively correlated with the strength of concrete and steel while negatively correlated with the porosity and the angle of the internal porous steel plate.

The empirical formulas were presented.

This study [20] focused on investigating the shear performance and failure mechanisms of stud shear connectors within steel-fiber-reinforced-concrete composite beams, compared to their counterparts in steel-normal-strength-concrete composite beams. Notably, the experimental findings unequivocally identified stud shearing failure as the predominant failure mode in all pushout specimens. A key observation arising from this research was the efficient mitigation of crack development in the steel fiber-reinforced cementitious composite beams, which could be attributed to the incorporation of high-strength steel fibers into the normal concrete. To further analyze and validate these outcomes, a finite element model was developed and calibrated using pushout test results. The results of the finite element analysis highlighted a noteworthy enhancement in the shear resistance of stud shear connectors with increasing concrete compressive strength, stud diameter, and tensile strength. Conversely, the aspect ratio of the studs was found to exert a relatively minor influence on the ultimate resistance of stud shear connectors. In conclusion, empirical formulas were presented, consolidating the research's findings and providing practical insights into the behavior of these connectors in composite beams.

In study [21], an examination was conducted on steel lightweight aggregate-concrete composite beams featuring bolted shear connections, with a comparison made to normal concrete composite beams. A three-dimensional numerical model was meticulously developed for the purpose of investigating the shear characteristics of the bolt connections integrated into steel lightweight aggregate-concrete composite beams. This modeling effort took into account nonlinear geometric effects and material nonlinearities to ensure a comprehensive analysis. To establish the credibility and accuracy of the finite element modeling, an initial calibration and validation process was undertaken, employing data from push-off tests described in existing literature. Within the scope of this research, the fundamental shear properties of the bolted connections were scrutinized. Additionally, the study delved into the influence of concrete strength, concrete density, bolt diameter, and bolt tensile strength on the shear behavior of the bolt connections embedded within steel lightweight aggregate-concrete composite beams. In light of the findings, the research culminated in the proposal of design formulae, offering valuable insights for engineers and designers engaged in the domain of steel lightweight aggregate-concrete composite beams and bolted shear connections.

The research paper [22] introduces a bolted nail and a combined connector designed to mitigate the impact of various factors on the mechanical performance of shear stress connectors. Through a

 doi:10.20944/preprints202312.2029.v1

series of experimental investigations, the study explores these connectors' shear resistance, failure mechanisms, and stress-strain characteristics. A comparative analysis between the bolt connectors and standard stud connectors reveals that stud connectors exhibited signs of deformation at 64% of the bolted connectors' ultimate capacity. In contrast, bolted connectors displayed deformation at 56% of their maximum capacity. The onset of connector cracking occurred when the included angle with the horizontal direction reached approximately 45° for bolted connectors and about 50° for stud connectors. Notably, stud connectors exhibited excellent shear resistance and ductility. Unlike bolted connectors, stud connectors demonstrated higher initial deformation bearing capacity and ultimate bearing capacity, surpassing the former by 27.68% and 12.07%, respectively. Furthermore, stud connectors exhibited superior ductility, deformation performance, and shear resistance. On the other hand, bolted connectors excelled in pull-out resistance.

A numerical model pertaining to bearing-shear connectors was meticulously crafted and subsequently validated through a series of pushout tests [23]. The primary focus was to investigate the stress distribution within the bearing-shear connectors and the accompanying concrete slab during loading, with a particular emphasis on unraveling the failure mechanisms inherent to these connectors. Notably, the shear behavior of the bearing-shear connectors was found to be notably influenced by key parameters, including the concrete strength, thickness of the shear plate, and its tensile strength. Insights gained from experimental data and numerical analysis culminated in the formulation of calculation formulae for both the ultimate shear resistance and the slip modulus, which serve as valuable tools for understanding and predicting the performance of bearing-shear connectors.

The study [24], [25] delved into the flexural and shear-bonding characteristics of the developed composite beams, drawing from experimental investigations and theoretical and analytical research. Seven flexural beams underwent testing involving the application of monotonic bending loads at two support points to elaborate on the methodology. In addition, four shear bonding beams were subjected to compressive loading procedures. The findings from the flexural tests unveiled a noteworthy trend wherein the flexural strength of the broader composite-steel beams exhibited an approximate 20% enhancement as the steel thickness increased by 3 mm, transitioning from 6 mm to 9 mm. In the context of shear-bonding tests, it was established that all specimens lacking shear connectors displayed inadequate shear-bonding strength to withstand the mechanical bonding mechanism. Consequently, it was suggested that such specimens necessitate reinforcement in the form of two or more flat bars.

The study [26] delved into the examination of precast steel-ultra-high-performance concrete (UHPC) composite beams that were equipped with high-strength friction-grip bolt (HSFGB) shear connectors. A finite element model was meticulously crafted, considering the inherent nonlinearities of materials and geometry. Through empirical validation, this model was confirmed for its accuracy and reliability. Subsequently, the research unveiled the intricate mechanisms governing the internal stress transfer processes of HSFGBs and elucidated the failure mechanism inherent in precast UHPC.

An analysis of articles devoted to assessing the strength of the contact joint of steel-reinforced concrete structures in recent years shows that they are mainly devoted to developing and experimental studies of various anchor connections. The bearing capacity of a contact joint is evaluated either based on the Eurocode or various computer programs using the finite element method, which cannot lead to reliable and economical solutions. The purpose of this article is to assess the strength of the most common types of anchor ties based on analytical dependencies, to achieve which the tasks of experimental and numerical studies are set, based on them, the formulation of formulas reflecting the actual stress-strain state of shear stud bonds.

2. Materials and Methods

Numerous experimental and theoretical studies by many authors have revealed the stress-strain state of the contact weld in depth and width. The dependencies reflect the geometric parameters and strength properties of materials. The scientific results obtained over many years are reflected in many countries' Eurocode and regulatory documents. The following methods are used to determine the

Preprints (www.preprints.org) | NOT PEER-REVIEWED | Posted: 27 December 2023 doi:10.20944/preprints202312.2029.v1

load-bearing capacity of vertical circular shear stud bonds. The bearing capacity of concrete according to the code [27] is determined as

$$P_{rd} = 0.24ld_{an}\sqrt{10R_b}\ ;\ 2.5 \le l/d_{an} \le 4.2\,, \tag{1}$$

$$P_{rd} = d_{an}^2\sqrt{10R_b}\ ;\ l/d_{an} \ge 4.2\,, \tag{2}$$

where l/d_{an} is means shear studs bond length and diameter; R_b is indicates the calculated concrete resistance.

The bearing capacity of the shear studs bond could be determiner in accordance to the material of the steel shear stud bonds [27]:

$$P_{an} = 0{,}063d_{an}^2\gamma_c R_y\,, \tag{3}$$

where γ_c is the value of the coefficient of working conditions, R_y is the value estimated shear studs bond resistance.

The bearing capacity of an inclined shear studs bond made of round reinforcing steel or identical shear studs bond branches in the form of an inclined yoke is proposed to be determined by the formula:

$$P_{an} = 0.1A_{an}\gamma_c R_y\cos\alpha + d_{an}^2\sqrt{10R_b\sin\alpha}\,, \tag{4}$$

Eurocode [28] proposes to take into account the work of the shear studs bond in tension by the expression

$$P_{rk} = 0{,}8A_b f_u\ , \tag{5}$$

where f_u is the limiting average resistance of the shear studs bond to treatment.

The research explores the adjustment of shear stud bond bearing capacity, as advocated by British and New Zealand codes, through the introduction of coefficients into the relevant formulas. Additionally, studies conducted at the Hong Kong Polytechnic University involved the investigation of steel-reinforced concrete samples equipped with various stud bolts. These studies comprehensively assessed the performance of these stud bolts in both shear and tension, considering cases where shear forces were applied perpendicular to the shear stud bonds (direct shear) and at an angle (combined shear) [8].

Steel-reinforced concrete prisms in a numerical experiment were modeled using the ANSYS software for samples with geometric parameters and loading according to the schemes corresponding to experimental studies. In a numerical experiment using a software package, calculations were performed in three stages: at the first stage, the finite element base of the prism sample was modeled; at the second stage, the loading conditions and physical and mechanical properties of the model were recorded; at the third stage, the complex of equations was solved by the finite element method.

The following types of samples are considered (Figure 1): b) prisms with shear stud bonds from vertical rods; c) samples with shear stud bonds from loop-shaped collars; d) models with anchors made of steel plates.

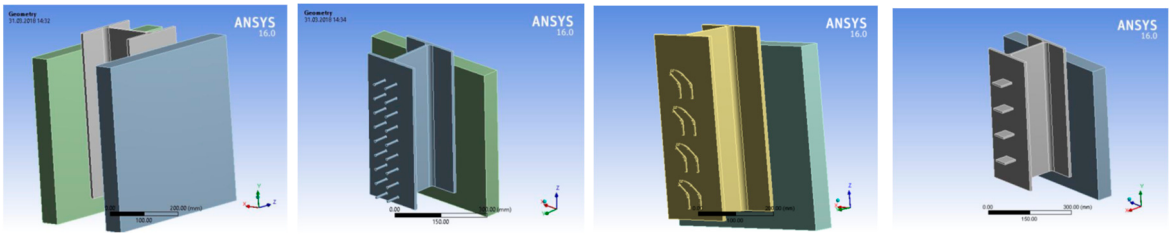

a) b) c) d)

Preprints (www.preprints.org) | NOT PEER-REVIEWED | Posted: 27 December 2023 doi:10.20944/preprints202312.2029.v1

Figure 1. a) General view of the prism model; b) shear stud bonds from reinforcing bars; c) anchors from loop-shaped collars; d) shear studs bond from steel plates.

Between the surface of the concrete slab (concrete class B30) and the surface of the steel belt of the I-beam (steel class C245), a frictional contact with k-0.45 was specified. Rough gives the contact between the shear stud bonds and the concrete of the slab. This contact implies a possible separation of the surface and corresponds to an infinite coefficient of friction between the bonding bodies.

In a numerical experiment, steel-reinforced concrete prisms were modeled using ANSYS according to a scheme corresponding to experimental studies. During the numerical experiment, using the software package, calculations were performed in three stages: at the first stage, a finite element model of the prism sample was simulated, at the second stage, the necessary loading conditions and physical and mechanical properties of the model were recorded, at the third stage, a set of equations was solved using the finite element method.

Next, the calculations were performed with the properties and conditions specified above, and a mosaic of stresses and strains was obtained. Figure 2 shows the stress pattern and strains in anchor ties of various types.

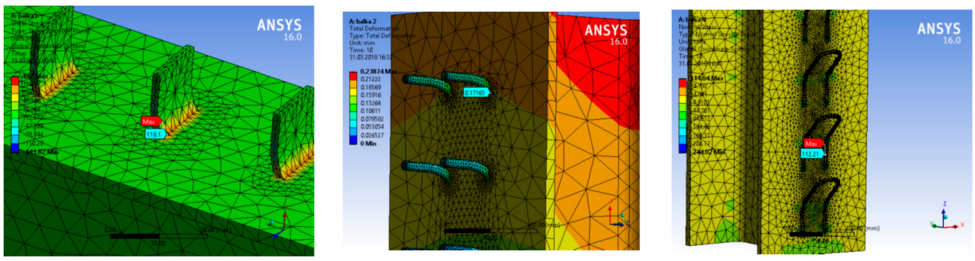

Figure 2. Mosaic of stresses and strains in anchors.

Models from prisms with a symmetrical arrangement of concrete slabs on the side of a steel I-beam's shelves and combined by anchors were subjected to numerical and natural studies. The materials of the steel I-beam and concrete slab, as well as anchor rods, were taken from the most commonly used steel and concrete in steel-reinforced concrete floors. Welding anchor rods to the shelves of the I-beam embedment of concrete slabs was conducted in laboratory conditions. The dial gauges were used (Figure 3a). The tests were carried out using an IPS-200 power press to measure the shear of layers.

Models of prisms were made for experimental studies using the results of numerical studies. The I-beam made of C245 steel, reinforcing bars, and plates from A500 were used for the models. The concrete class was B30. Samples were made with vertical rods, inclined loop-shaped clamps, and steel plates with different spacing between them.

Experimental studies of reinforced concrete prisms and beams for static and repeated static loads [6] make it possible to establish the actual bearing capacity of the contact connection, as well as the nature of the formation and development of cracks in beams or ceilings, features of shear layers, the operation of anchors both in the elastic stage and beyond the elastic limit.

In experimental studies of prism models, to ensure the symmetry of the shift of the layers, mainly I-beams made of steel C245 were used. As anchors, angles, plates, loop-shaped clamps, and reinforcing bars from A500 were used, and concrete of class B30 was used in the slabs. The pitch of anchors varied f in beams from 150 to 300 mm [6].

Preprints (www.preprints.org) | NOT PEER-REVIEWED | Posted: 27 December 2023 doi:10.20944/preprints202312.2029.v1

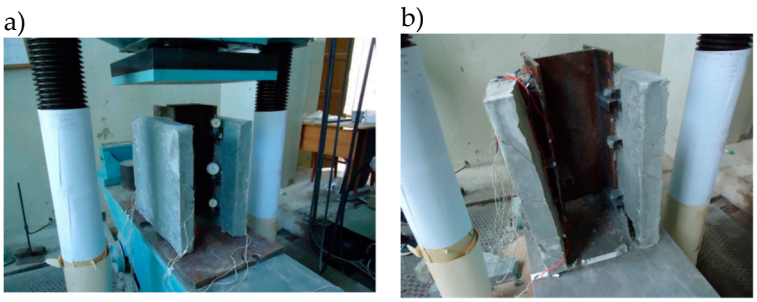

Figure 3. Steel-reinforced concrete prisms in installation (a), and after testing (b).

The prisms were tested in the Kazan State University of Architecture and Civil Engineering laboratory, Kazan, Russia. An IPS-200 hydraulic press created the load. During the test, the deformations of the concrete flange, I-beam steel, and anchor ties were measured using strain gauges glued to the surface of the concrete, beam, and anchor. Deformations of concrete and steel were recorded by strain gauges with bases of 50 mm and 20 mm, respectively. The shift of layers was measured with I4 dial indicators (Figure 3a).

A trial test was first carried out with a force of 4.9 kN After taking readings from all instruments to check the performance of the testing system. After reviewing the system, the test was done by loading in steps of 8.9 kN from the expected breaking load. At the stages during exposure, indicators were taken from strain gauges, I4, i.e., concrete and steel deformations and movements were recorded.

The breaking load was recorded according to the readings of the test press scale at the moment of physical destruction of the sample. The maximum load value was taken to be the load at which complete physical destruction of the samples occurred. The development of cracks in the body of the side slab was mainly observed before failure. The destruction occurred from separating a concrete slab from a steel I-beam. Figure 3b shows the general appearance and nature of the destruction.

3. Results and Discussion

3.1. Experimental data

Figure 4 shows the graphs of the relative dependences of stresses on load and relative deformations for three types of anchors. An analysis of the graphs of relative deformations for different anchors (Figure 5b) shows the best performance of vertical anchors; that is, they have an increased bearing capacity than plates and loop anchors by 1.7 and 2.5 times, and the relative deformations of vertical anchors are four times greater than loop anchors, which shows better joint work with the slab without the appearance of fracture cracks in the concrete.

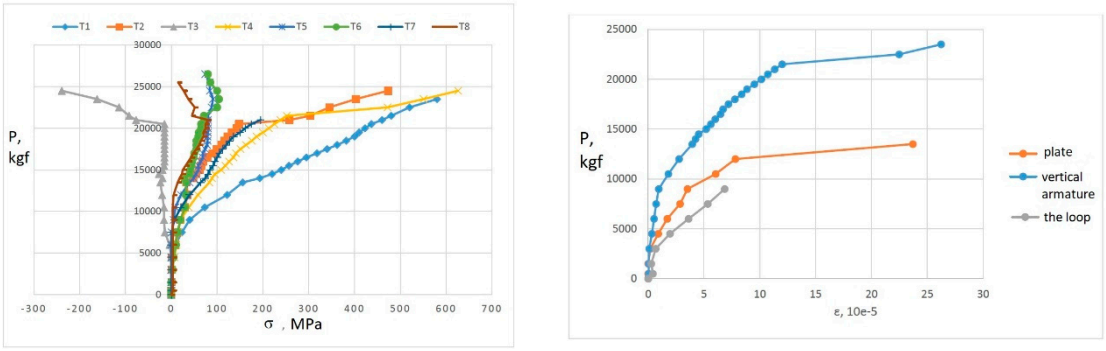

a) b)

Figure 4. Dependences of stresses for vertical anchor rods (a), relative deformations for three types of anchors (b).

Preprints (www.preprints.org) | NOT PEER-REVIEWED | Posted: 27 December 2023 doi:10.20944/preprints202312.2029.v1

Figure 5 shows the graphs of the vertical anchors' deformations dependences, depending on the pitch, and the graphs of relative deformations comparison for different anchor types. Dependence graphs of vertical anchors for different pitches (50, 75, 100mm) show that anchors with a pitch of 50mm provide better joint work with concrete, and with an anchor pitch of 100mm, the bearing capacity of the sample is 2.33 times lower than the other two, and the deformability is five times more. A sample equipped with rod anchors with a pitch of 50 mm up to 240 kN works elastically and later in the plastic stage.

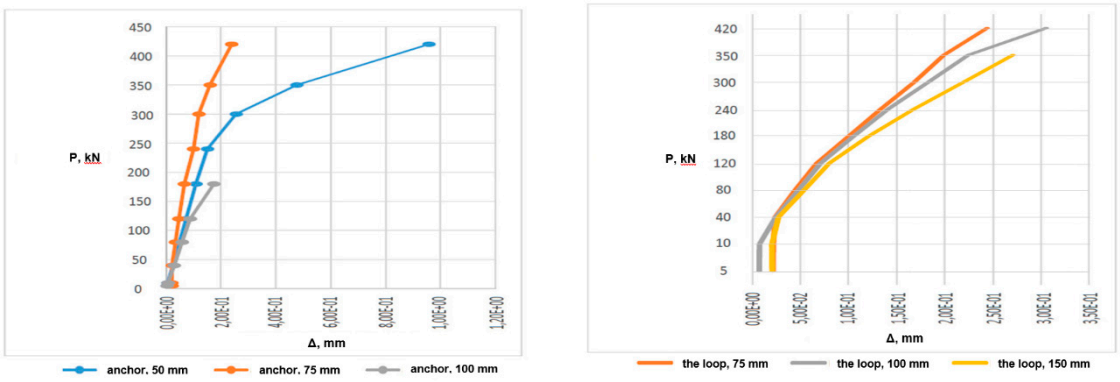

a) b)

Figure 5. Dependences of deformations for vertical anchors a), comparison of deformations for three types of anchors b).

Figure 6 shows the load-stress graphs for those types of anchors and compares the results of numerical and natural experiments.

The following tasks are usually solved for contact weld designing and calculating:

- the shear forces arising in the contact seam of the bent structures are determined;
- the bearing capacity of the contact seam is determined.

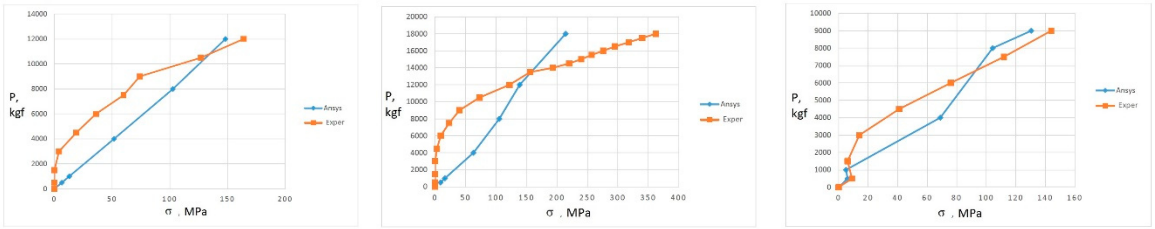

Figure 6. Comparison of the results of numerical and natural experiments, "load-stress" graphs for different types of anchors.

The presence in the structure of a composite steel-reinforced concrete structure of layers (reinforced concrete slabs and steel beams) with pronounced distinctive features in terms of physical and mechanical properties imposes increased requirements on anchor devices, on the one hand, reliable in terms of bearing capacity, on the other hand, technologically advanced in execution. At the stage of anchor ties choosing, their critical analysis is required from the standpoint of shear work and material efficiency. It is also necessary to find ways to evaluate the strength corresponding to their actual bearing capacity for operational loads.

At the layers junction - a reinforced concrete slab and a steel beam, the stress-strain state of the connection is very complex, connected on the one hand with crushing, and sometimes with chipping of concrete, and on the other hand, with bending of the steel anchor and its tensile work [7]. The bearing capacity of the contact weld must be determined taking into account all factors, the operation of the weld elements, taking into account their actual stress-strain state.

Our experimental studies and those of other authors show that at the junction of the layers of a reinforced concrete slab and a steel beam, there is a rather complex stress-strain state; at the limit

Preprints (www.preprints.org) | NOT PEER-REVIEWED | Posted: 27 December 2023 doi:10.20944/preprints202312.2029.v1

state, the slab collapses with the opening of cracks or crushing of concrete, and the steel anchor experiences bending with tension. When analytically determining bearing capacity, all these factors must be considered in analytical research.

3.2. Analytical research

The inclined anchor staple-like figurative bonds mainly work in tension, and the concrete at the contact experiences tension and shearing. Concrete spalling can be significantly reduced by rational placement and configuration of anchors. The case of anchor staple-like shaped inclined clamp and concrete in contact with it is the most significantly affecting the bearing capacity of the contact seam. Assuming that the concrete is subjected to tension along the entire length of the anchor rod evenly, the magnitude of the shear force perceived by the concrete T_b has the form:

$$T_b = \sigma_b\left(\varepsilon_b\right) l_x \pi d_a \cos\alpha, \tag{6}$$

where α, l_x, d_a are the angle of inclination, the length, and the diameter of the staple-like of the figurative anchor connection. In case of destruction along concrete $\sigma_b\left(\varepsilon_b\right)$ is equal to Rb, and in case of destruction along the anchor rod, the stresses in concrete are determined on the assumption that the concrete deformations are equal to the maximum elongation of the inclined anchor rod.

The value of the limiting shear force perceived by the anchor connection, assuming the anchor behavior tension, is as follows:

$$T_s = \sigma_s\left(\varepsilon_s\right)\frac{\pi d_a^2}{4}\cos\alpha. \tag{7}$$

The main purpose of anchors in steel-reinforced concrete structures is to prevent the shear of layers - plates and steel beams. They must perceive the shear force T arising from the transverse forces in the bending element, which can be determined by the formula [8]

$$T = QS_{pl} / J_{red} \cdot a, \tag{8}$$

where Q is the transverse force, Spl is the static moment of the plate relative to the neutral axis of the combined section, Jred is the moment of inertia of the reduced section, a - is the pitch of the anchors.

The connection strength of a concrete shelf with a steel beam is determined from the condition

$$T \le T_{ult};\ T_{ult} = \min\left(T_b; T_s\right). \tag{9}$$

Experimental studies of steel concrete specimens with round vertical anchor rods have shown depending on the anchor diameter and the magnitude of the shear force T, stress diagrams in the rod can be triangular (elastic work), rectangular (plastic work), mixed (elastic-plastic work) (Figure 8). The stresses diagram in concrete along the length of the anchor rod has a curvilinear outline (Figure 7), however, for the sake of simplicity of writing formulas in calculations, the calculation diagram of a rectangular or triangular outline is often taken [7].

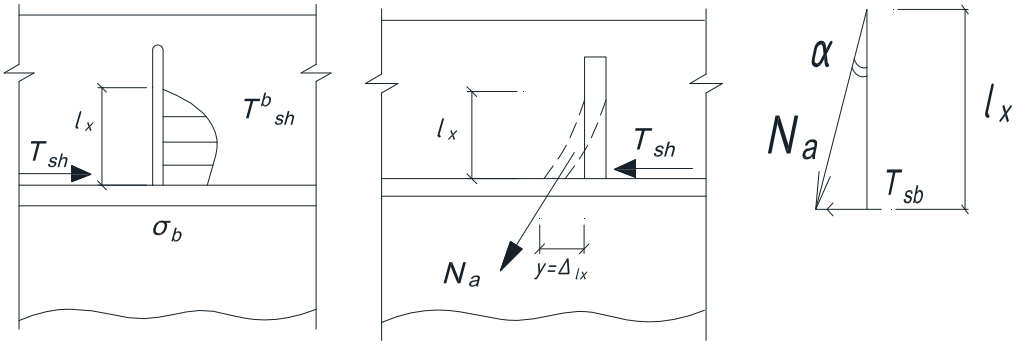

Preprints (www.preprints.org) | NOT PEER-REVIEWED | Posted: 27 December 2023 doi:10.20944/preprints202312.2029.v1

Figure 7. Concrete stresses along the tie rod, tie rod deflection, and force diagram.

Vertical anchor connection of steel-reinforced concrete flexural elements is subjected to bending and tension. Here, the shear force is determined from the stress-strain state consideration of the slab with ribs. The shear force was found in a vertical anchor rod by considering it as a cantilever [29].

The vertical anchor rod was considered in the form of a cantilever, so the shear force is:

$$T_s = M_s / l_s \,. \tag{10}$$

The tensile force in the anchor rod is determined from:

$$N_a = T_s / \sin\alpha \,. \tag{11}$$

From the equilibrium condition of moments from external and internal forces, considering the stress diagram in concrete as an external component for a vertical anchor was obtained:

a) for triangular stress diagrams of concrete and anchor rod (Figure 8) [8].

$$T_s = 3/8 \frac{\sigma_s(\varepsilon_s) A_s \omega}{l_x} d_s n\,; \tag{12}$$

where n is the number of anchor rods in the considered section, ω is the plot completeness factor.

b) for a triangular diagram of concrete and a rectangular diagram of stresses in the anchor

$$T_s = 3/4 \frac{\sigma_s(\varepsilon_s) A_s \omega}{l_x} d_s n\,; \tag{13}$$

c) for rectangular stress diagrams of concrete and anchor rod

$$T_s = 1/2 \frac{\sigma_s(\varepsilon_s) A_s \omega}{l_x} d_s n\,; \tag{14}$$

d) for a curvilinear diagram of concrete and a rectangular diagram of anchor stresses

$$T_s = 1/4 \frac{\sigma_s(\varepsilon_s) A_s \omega}{y(l_x)} d_s n\,, \tag{15}$$

where $y(l_x)$ is the distance to the center of the plot.

Obviously, under the joint action of M and N, the plasticity hinge formation will occur at lower values of forces than when they are considered as separate actions.

Obviously, under the joint action of M and N, the plasticity hinge formation will occur at lower values of forces than in considering M and N as separate actions.

With a gradual increase in the external force (M and N), the stress diagrams in the anchor section, passing through the stages shown in Figure 8, the limiting diagram with a plasticity hinge is reached, shifted relative to the axis of the anchor rod (Figure 9) In this case, it can be assumed that the moment is perceived by an internal pair of forces formed from equal areas of the compressed and stress diagram stretched zones, and the longitudinal force - the middle, symmetrical part of the stress diagram, marked in Figure 9).

Based on the condition of the joint action of M and N, the value of the limiting moment of the tensile-bent rod of the round-section anchor are as follows:

$$M_{\lim}^{N} = F\xi d = \sigma_T A_{seg} \xi d = \sigma_T \frac{\pi c(1-\xi) d}{4} \xi d = \sigma_T \frac{\pi c}{4} d^2 \xi (1-\xi)\,. \tag{16}$$

Here *Aseg* is the areas of segment:

Preprints (www.preprints.org) | NOT PEER-REVIEWED | Posted: 27 December 2023 doi:10.20944/preprints202312.2029.v1

$$A_{seg} = \frac{\pi cb}{4};\ c = 2\sqrt{2br - b^2}\ . \tag{17}$$

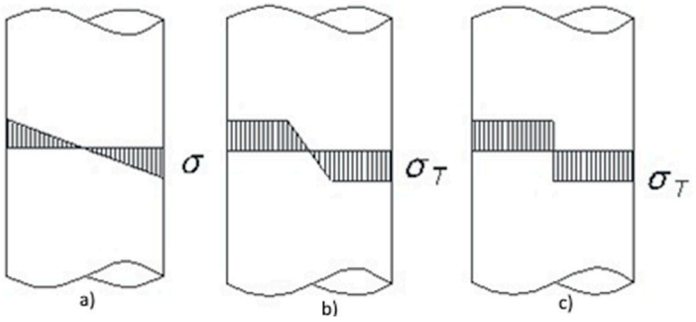

Figure 8. Stress state of the bent anchor rod: a) elastic, b) elastic-plastic, c) plastic work.

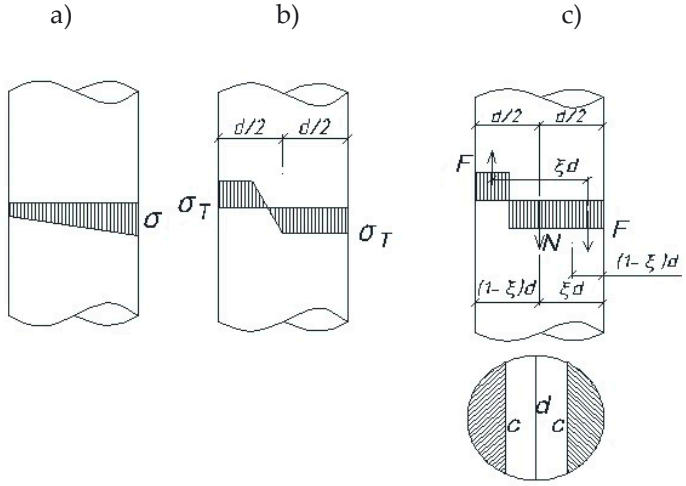

Figure 9. Stresses diagrams of a tensile-bent anchor rod.

The limiting longitudinal force of a tensile-bent anchor of a circular cross-section is written in the form:

$$N_{\lim}^{M} = \sigma_T \left(\frac{\pi d^2}{4} - 2\frac{\pi c}{4}(1-\xi)d \right) = \sigma_T \frac{\pi c(1-\xi)d}{4} \xi d = \sigma_T \frac{\pi d}{4}[d\ - 2c(1-\xi)]; \tag{17}$$

$$\nu = \frac{N_{\lim}^{M}}{N_T} = \frac{\sigma_T\, \pi d/4[d - 2c(1-\xi)]}{\sigma_T \pi d^2/4} = \frac{d - 2c(1-\xi)}{d} = 1 - \frac{2c}{d}(1-\xi)\,; \tag{18}$$

$$\mu = \frac{M_{\lim}^{N}}{W_{pl}\sigma_T} = \frac{5M_{\lim}^{N}}{\pi d^3 \sigma_T} = 5/4\pi c \frac{\xi(1-\xi)}{d}, \tag{19}$$

where ξd is the neutral line's relative distance from the anchor section's edge.

The equation of the boundary curve that determines the destruction area (achievement of the plasticity hinge) from the area of anchor rod safe operation under the simultaneous action of M and N

$$\nu^2 + \mu = 1;\ \text{ or } \left(\frac{N_{\lim}^{M}}{N_T} \right)^2 + \left(\frac{M_{\lim}^{n}}{M_T} \right) = 1\,. \tag{20}$$

 doi:10.20944/preprints202312.2029.v1

The formula checks the strength of the vertical anchor rod:

$$\left(\frac{N}{AR_{an}}\right)^2+\frac{M}{W_{pl}R_{an}}\le 1. \quad (21)$$

When the concrete slab is shifted relative to the upper chord of the steel beam, the anchor rod bends in the concrete mass, and due to significant displacements of the layers, the anchor rod stretches (Figure 7). Many researchers note the head detachment of a stud bolt under extreme loads. To prevent head detachment the calculation of the stud bolt subjected to bending with tension is carried out taking into account the bending moment and tensile forces taking into account tensile forces and bending moment.

4. Conclusions

1. The stress-strain state strength assessment for methods anchor ties of steel-reinforced concrete structures are analyzed.

2. Calculations were made on the ANSYS PC for steel-reinforced concrete prisms, which made it possible to reveal the stress-strain state pattern of the contact joint, the stages of cracks, the development of plastic deformations in the concrete flange and in anchor ties.

3. The features of the stress-strain state of steel-reinforced concrete samples with different anchor ties for static loads were studied, which showed:

- in vertical rod anchors, the onset of plastic deformation corresponds to loads twice as high as in lamellar anchors, which can be explained by the better joint work steel-concrete in these samples;
- the largest movements for prisms with vertical anchors than for samples with plate anchors (less than 1.5 times) and with loop-shaped anchors (less than two times);
- the destruction of concrete slabs occurs mainly along the cut line by anchor devices, and destruction begins from the formation of cracks from the separation of the contact and from the development of the plastic deformation in anchor connections;
- the bearing capacity of prisms with vertical anchor rods is 37% and 49% higher, respectively, than prisms with loop and plate anchors.

The numerical calculations carried out according to domestic standards SP266.1325800.2016 show that the bearing capacity of the contact seam with anchor ties is 18-23% less than the experimental data.

4. Field tests showed:

- in plate anchors, plastic deformations began when the load reached 117.7 kN, and in vertical anchors, plastic deformations began when the load reached 220.6 kN;
- the largest displacements were obtained: for prisms with looped anchors of 1.5 mm, for prisms with plates of 2.2 mm, for prisms with vertical anchors of 2.849 mm;
- the concrete slab destruction of prisms occurs from the contact separation, mainly along the cut line by anchor devices and from the development of the plastic deformation in anchor ties;

5. The analytical dependencies are proposed to assess the contact strength between the slab and the beam, considering the tensile and bending forces.

Author Contributions: Conceptualization, F.Z. and A.T.; methodology, F.Z. and A.T.; software, F.Z. and A.T.; validation, F.Z. and A.T.; formal analysis, F.Z. and A.T.; investigation, F.Z. and A.T.; resources, F.Z. and A.T.; data curation, F.Z. and A.T.; writing—original draft preparation, F.Z. and A.T.; writing—review and editing, F.Z. and A.T.; visualization, F.Z. and A.T.; supervision, F.Z. and A.T.; project administration, F.Z. and A.T. All authors have read and agreed to the published version of the manuscript.

Data Availability Statement: The data available on request.

Conflicts of Interest: The authors declare no conflict of interest.

References

1. Benedetty, C.A.; dos Santos, V.B.; Krahl, P.A.; Rossi, A.; Silva, F. de A.; Cardoso, D.C.T.; Martins, C.H. Flexural and shear behavior of steel-UHPC composite beams: a review. *Eng. Struct.* 2023, *293*.
2. Ranzi, G.; Leoni, G.; Zandonini, R. State of the art on the time-dependent behaviour of composite steel-concrete structures. *Vol. 80, Pages 252 - 263* **2013**, *80*, 252–263. https://doi.org/10.1016/j.jcsr.2012.08.005.
3. Jurkiewiez, B.; Hottier, J.M. Static behaviour of a steel-concrete composite beam with an innovative horizontal connection. *J. Constr. Steel Res.* **2005**, *61*, 1286–1300. https://doi.org/10.1016/j.jcsr.2005.01.008.
4. Jurkiewiez, B.; Braymand, S. Experimental study of a pre-cracked steel-concrete composite beam. *J. Constr. Steel Res.* **2007**, *63*, 135–144. https://doi.org/10.1016/j.jcsr.2006.03.013.
5. Jurkiewiez, B. Static and cyclic behaviour of a steel-concrete composite beam with horizontal shear connections. *J. Constr. Steel Res.* **2009**, *65*, 2207–2216. https://doi.org/10.1016/j.jcsr.2009.06.018.
6. Ernst, S.; Bridge, R.Q.; Wheeler, A. Correlation of Beam Tests with Pushout Tests in Steel-Concrete Composite Beams. *J. Struct. Eng.* **2010**, *136*, 183–192. https://doi.org/10.1061/(asce)0733-9445(2010)136:2(183).
7. Henderson, I.E.J.; Zhu, X.Q.; Uy, B.; Mirza, O. Dynamic behaviour of steel-concrete composite beams with different types of shear connectors. Part I: Experimental study. *Vol. 103, Pages 298 - 307* **2015**, *103*, 298–307. https://doi.org/10.1016/j.engstruct.2015.08.035.
8. Henderson, I.E.J.; Zhu, X.Q.; Uy, B.; Mirza, O. Dynamic behaviour of steel-concrete composite beams with different types of shear connectors. Part II: Modelling and comparison. *Eng. Struct.* **2015**, *103*, 308–317. https://doi.org/10.1016/j.engstruct.2015.08.033.
9. Henderson, I.E.J.; Zhu, X.Q.; Uy, B.; Mirza, O. Dynamic behaviour of steel-concrete composite beams retrofitted with various bolted shear connectors. *Eng. Struct.* **2017**, *131*, 115–135. https://doi.org/10.1016/j.engstruct.2016.10.021.
10. Colajanni, P.; La Mendola, L.; Monaco, A. Review of push-out and shear response of hybrid steel-trussed concrete beams. *Buildings* 2018, *8*.
11. Al-Shuwaili, M.A.; Palmeri, A.; Lombardo, M. Experimental characterisation of Perfobond shear connectors through a new one-sided push-out test. In Proceedings of the Procedia Structural Integrity; Elsevier {BV}, 2018; Vol. 13, pp. 2024–2029.
12. Molkens, T.; Dobrić, J.; Rossi, B. Shear resistance of headed shear studs welded on welded plates in composite floors. *Eng. Struct.* **2019**, *197*, 109412. https://doi.org/10.1016/j.engstruct.2019.109412.
13. He, J.; Suwaed, A.S.H.; Vasdravellis, G.; Wang, S. Behaviour and design of the 'lockbolt' demountable shear connector for sustainable steel-concrete composite structures. *Structures* **2022**, *44*, 988–1010. https://doi.org/10.1016/j.istruc.2022.08.062.
14. Ling, Y.; Zheng, Z.; Yang, T.Y.; Ma, H. Behaviour and Modeling of the Bearing Capacity of Shear Stud Connectors. *Int. J. Steel Struct.* **2019**, *19*, 650–659. https://doi.org/10.1007/s13296-018-0154-3.
15. Chen, J.; Wang, W.; Ding, F.X.; Xiang, P.; Yu, Y.J.; Liu, X.M.; Xu, F.; Yang, C.Q.; Long, S.G. Behavior of an advanced bolted shear connector in prefabricated steel-concrete composite beams. *Materials (Basel).* **2019**, *12*. https://doi.org/10.3390/ma12182958.
16. Thangasamy, L.; Kandasamy, G. Behavior of steel-coconut shell concrete-steel composite beam without and with shear studs under flexural load. *Materials (Basel).* **2020**, *13*. https://doi.org/10.3390/MA13112444.
17. Wang, W.; Zhang, X.-D.; Ding, F.-X.; Zhou, X.-L. Finite element analysis on shear behavior of high-strength bolted connectors under inverse push-off loading. *Energies* **2021**, *14*. https://doi.org/10.3390/en14020479.
18. Karimipour, A.; Ghalehnovi, M.; Golmohammadi, M.; de Brito, J. Experimental investigation on the shear behaviour of stud-bolt connectors of steel-concrete-steel fibre-reinforced recycled aggregates sandwich panels. *Materials (Basel).* **2021**, *14*. https://doi.org/10.3390/ma14185185.
19. Li, C.; Cao, H.; Guan, D.; Li, S.; Wang, X.; Soloveva, V.Y.; Dalerjon, H.; Fan, Z.; Qin, P.; Liu, X. Study on Mechanical Properties of Multi-Cavity Steel-Concrete Composite Beam. *Materials (Basel).* **2022**, *15*. https://doi.org/10.3390/ma15144882.
20. Peng, K.; Liu, L.; Wu, F.; Wang, R.; Lei, S.; Zhang, X. Experimental and Numerical Analyses of Stud Shear Connectors in Steel–SFRCC Composite Beams. *Materials (Basel).* **2022**, *15*. https://doi.org/10.3390/ma15134665.
21. Wang, W.; Zhang, X.; Ren, Y.; Bai, F.; Li, C.; Li, Z. Finite Element Modelling of Bolt Shear Connections in Prefabricated Steel Lightweight Aggregate–Concrete Composite Beams. *Buildings* **2022**, *12*. https://doi.org/10.3390/buildings12060758.
22. Ma, S.; Lou, Y.; Bao, P. Experimental research and numerical analysis of shearing resistance in steel-concrete composite beam connectors. *Case Stud. Constr. Mater.* **2022**, *17*, e01210. https://doi.org/10.1016/j.cscm.2022.e01210.
23. Zheng, Z.; Zou, Y.; Chou, Y.; Qin, F.; Chen, F.; Di, J.; Zhang, Z. Shear Behaviour and Calculation Methods of Bearing-Shear Connectors for Prefabricated Steel–Concrete Composite Beams. *Materials (Basel).* **2023**, *16*. https://doi.org/10.3390/ma16134616.

24. Choi, Y.C.; Kim, J.Y.; Lee, K.S.; Jung, J.S. Experimental study on structural performance of new steel-concrete composite beam for both long-span and low-height parking structures. *J. Asian Archit. Build. Eng.* **2023**, *22*, 1028–1049. https://doi.org/10.1080/13467581.2022.2044822.
25. Choi, Y.C.; Lee, B.G.; Lee, K.S.; Park, K.S.; Jung, J.S. Experimental Study on Structural Performance of New Steel–Concrete Composite Beam for Both Long-Span and Low-Height Parking Structures. *Int. J. Steel Struct.* **2023**, *23*, 417–430. https://doi.org/10.1007/s13296-022-00702-2.
26. Fang, Z.; Hu, L.; Jiang, H.; Fang, S.; Zhao, G.; Ma, Y. Shear performance of high-strength friction-grip bolted shear connector in prefabricated steel–UHPC composite beams: Finite element modelling and parametric study. *Case Stud. Constr. Mater.* **2023**, *18*, e01860. https://doi.org/10.1016/j.cscm.2023.e01860.
27. Russian Construction Code SP 266.1325800.2016 Composite steel and concrete structures. Design rules.
28. *EN 1992-1-1:2023 - Eurocode 2: Design of composite steel and concrete structures- Part 1-1: General rules and rules for buildings, bridges and civil engineering structures.;*
29. Odenbreit, C.; Nellinger, S. Mechanical model to predict the resistance of the shear connection in composite beams with deep steel decking. *Steel Constr.* **2017**, *10*, 248–253. https://doi.org/10.1002/stco.201710029.